Hindawi
Shock and Vibration
Volume 2023, Article ID 8829298, 19 pages
https://doi.org/10.1155/2023/8829298

Research Article

Detection, Localization, and Quantification of Damage in Structures via Artificial Neural Networks

Daniele Kauctz Monteiro,[1] **Letícia Fleck Fadel Miguel**,[2] **Gustavo Zeni**,[3] **Tiago Becker**,[4] **Giovanni Souza de Andrade**,[5] **and Rodrigo Rodrigues de Barros**[5]

[1]*Postgraduate Program in Civil Engineering (PPGEC), Federal University of Rio Grande Do Sul (UFRGS), Porto Alegre, Brazil*
[2]*Department of Mechanical Engineering (DEMEC), Postgraduate Program in Mechanical Engineering (PROMEC), Postgraduate Program in Civil Engineering (PPGEC), Federal University of Rio Grande Do Sul (UFRGS), Porto Alegre, Brazil*
[3]*Postgraduate Program in Mining, Metallurgy and Materials Engineering (PPGEM), Federal University of Rio Grande Do Sul (UFRGS), Porto Alegre, Brazil*
[4]*Department of Mechanical Engineering (DEMEC), Federal University of Rio Grande Do Sul (UFRGS), Porto Alegre, Brazil*
[5]*Applied Mechanics Group (GMAp), School of Engineering, Federal University of Rio Grande Do Sul (UFRGS), Porto Alegre, Brazil*

Correspondence should be addressed to Daniele Kauctz Monteiro; daniele.kauctz@ufrgs.br

Received 8 June 2023; Revised 27 November 2023; Accepted 1 December 2023; Published 19 December 2023

Academic Editor: Xian-Bo Wang

This paper presents a structural health monitoring method based on artificial neural networks (ANNs) capable of detecting, locating, and quantifying damage in a single stage. The proposed framework employs a supervised neural network model that uses input factors calculated by modal parameters (natural frequencies or mode shapes), and output factors that represent the damage situation of elements or regions in a structural system. Unlike many papers in the literature that test damage detection methods only in numerical examples or simple experimental tests, this work also assesses the presented method in a real structure showing that it has potential for applications in real practical situations. Three different cases are evaluated through the methodology: numerical simulations, an experimental lab structure, and a real bridge. Initially, a cantilever beam and a 10-bar truss were numerically analyzed under ambient vibrations with different damage scenarios and noise levels. Afterward, the method is assessed in an experimental beam structure and in the Z24 bridge benchmark. The numerical simulations showed that the methodology is promising for identifying, locating, and quantifying single and multiple damages in a single stage, even with noise in the acceleration signals and changes in the first vibration mode of 0.015%. In addition, the Z24 bridge study confirmed that the damage detection method can localize damage in real civil structures considering only natural frequencies in the input factors, despite a mean difference of 4.08% between the frequencies in the healthy and damaged conditions.

1. Introduction

The presence of damage in civil structures, whether caused by natural deterioration processes or extreme events, can lead to their collapse causing accidents. Therefore, it is necessary to continuously monitor structures aimed at the user's safety and structural reliability. In this context, structural health monitoring (SHM) has become relevant in engineering for its perennial surveillance and analysis of systems. The term SHM is linked to vibration-based methods that involve observing the structure over time using the system's dynamic responses (displacements, velocities, and accelerations), with the structural condition being determined by damage-sensitive features. These properties include natural frequencies, frequency response function, mode shapes, mode shapes curvature, modal strain energy, and flexibility matrix (Ren et al. [1]).

Through the damage-sensitive features obtained over the useful life of the structure, several methods of damage detection can be employed according to the type of construction and its function. For instance, methods based on changes in modal parameters (Salawu [2], Allemang and Brown [3], Curadelli et al. [4]), modal parameter derivatives (Pandey et al. [5], Abdel Wahab and De Roeck [6], Cornwell et al. [7]), modal flexibility (Bernal [8], Miguel et al. [9]), Bayesian probabilistic inference (Sohn and Law [10], Zheng et al. [11]), wavelet transform (Liew and Wang [12], Altammar et al. [13]), matrix updating (Fadel Miguel et al. [14–16], Monteiro [17]), artificial neural network (ANN) (Wu et al. [18], Mehrjoo et al. [19]), and combination of techniques (Srinivas et al. [20], Shih et al. [21], Garcia-Perez et al. [22], Tran-Ngoc et al. [23]). State-of-the-art reviews on structural damage detection methods are presented by Doebling et al. [24], Fan and Qiao [25], and An et al. [26].

As damage detection methods generally use the comparison of information with the values obtained in the healthy condition (reference scenario), a methodology has better predictive capabilities when using physical parameters in the assessment process, such as numerical models. When a finite element (FE) model effectively represents the structure's dynamic properties, it can be adopted along with other techniques to identify damage. In this way, model-based and physics-informed methods have been deeply used in SHM employing machine learning (ML) algorithms, such as ANNs (Villalba and Laier [27]), support vector machines (Salkhordeh et al. [28]), and decision trees (Mariniello et al. [29]).

The approaches using the pattern recognition aspect within the ML discipline can predict and classify damage scenarios by interpolating relationships between data. Damage detection methods that use neural networks depend on the relations between input and output, in which a damaged state is estimated according to a set of damage-sensitive features that can be generated through a calibrated FE model or a hybrid approach (numerical and experimental data). For example, the first five natural frequencies of the structure or a set of wavelet coefficients can be used as input data to obtain damage location index as outputs (Farrar and Worden [30]).

According to Rytter [31], damage detection methods are classified into four levels: (1) damage detection, (2) damage localization, (3) damage quantification, and (4) prediction of the remaining service life of the structure. The methods available in the literature fall under levels 1 to 3, while level 4 is considered part of the structural assessment. However, there is still no widely accepted methodology for any structure or even any type of damage.

Generally, damage detection methods based on ANN do not achieve all Rytter's three levels (Hekmati Athar et al. [32]: level 1, Weinstein et al. [33]: levels 1 and 2, Xie et al. [34]: levels 1 and 2, Bisheh et al. [35]: level 1), or the authors propose multistage approaches to complete the three tasks (Malekjafarian et al. [36]: 2-stage method, Nick et al. [37]: 2-stage method). Detection typically involves identifying whether damage is present, followed by separate steps to locate the damage and quantify its severity. This fragmented approach may not fully capitalize on the relationship among these tasks, potentially resulting in suboptimal overall performance. Thus, a significant gap remains in approaches that seamlessly integrate the three critical tasks in a single stage.

In this context, this paper presents a framework for detecting, locating, and quantifying damage in structures via ANNs using natural frequencies and mode shapes identified from the responses to ambient excitation in a single stage. The main contribution of this work is a methodology easily applied to different structures using numerical data through a physics-informed neural network. A supervised learning algorithm is employed with input and output factors to represent the structure's modal properties and damage states, respectively.

Unlike many papers in the literature that test damage detection methods only in numerical examples or simple experimental tests, this work also evaluated the presented framework in a real structure, the Z24 bridge, showing that it has potential for applications in real practical situations. The proposed method is not only able to detect single and multiple damages but is also able to satisfactorily locate and quantify them, which is crucial to data-driven decision-making.

Three main steps are used to illustrate the presented framework in different structural applications: (1) numerical simulation of damage scenarios in two structures under ambient vibrations with different noise levels; (2) validation of the methodology through experimental testing in a lab system; and (3) application of the methodology in the Z24 bridge, a real benchmark structure. Thus, this paper is organized as follows. Section 2 presents the vibration-based damage detection method via artificial neural networks, Section 3 illustrates the numerical examples, Section 4 studies the experimental system, Section 5 presents the analysis of the Z24 bridge, and Section 6 presents the conclusions.

2. Damage Detection Method via Artificial Neural Networks

The damage detection method via neural networks presented in this paper builds a model that provides a relationship between modal parameters (input data) and structural properties (output data). This relationship between the data of a system is determined through a training process inspired by the structure and operation of the human brain. In this way, artificial neural networks try to reproduce human behaviors of learning, association, generalization, and abstraction. The interconnected processing elements (artificial neurons) perform simple operations and transmit their results to neighboring individuals.

An artificial neuron j has a set of inputs S_i (dendrites) and an output S_j (axon). The connections (synapses) formed between neurons have numerical values representing the strength of each bond. These values are called synaptic weights (w_i) and are used to store knowledge. With the formation of the neural network model, different input data are applied to each neuron, and these values are weighted by the weight of each synapse, as shown in Figure 1.

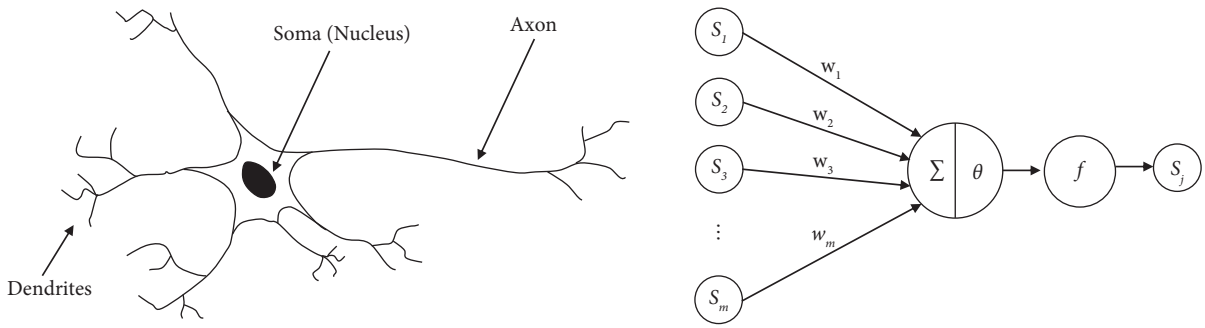

Figure 1: Artificial neuron model.

If the activity of a neuron reaches a certain value of the activation function f, the neuron propagates the received signal along the axon. The sum of the m inputs weighted by the respective synaptic weights adding a bias term θ_j defines the activation state:

$$S_j = f\left(\sum_{i=1}^{m} S_i w_i + \theta_j\right). \tag{1}$$

Each ANN can assume a different architecture according to its neuron's organization. The distribution of processing elements occurs in layers consisting of an input layer, an output layer, and one or more hidden layers. Thus, the number of existing layers and the number of elements in each form the architecture of a neural network.

The learning process can be divided into two algorithms: supervised learning and unsupervised learning. The learning algorithm is supervised when the training generates its results by labels of each set; i.e., there is a correct answer. However, when the input data are not linked with preestablished labels, the algorithm is unsupervised. While supervised learning applied in damage detection methods requires data from all possible damage scenarios, unsupervised learning only needs data from the system's normal condition (reference scenario). However, according to Farrar and Worden [30], it is not possible to diagnose damage scenarios beyond level 2 (location) in unsupervised learning. Therefore, in this work, supervised learning was used.

The training dataset for neural networks was obtained through numerical models, with the input data linked to the structural condition by identification, location, or quantification labels (output data). The database of each system was divided as follows: 70% for training, 20% for validation, and 10% for testing.

The input factors (IFs) were based on natural frequencies or mode shapes to detect damage by the ANN model. These modal parameters can capture essential characteristics of a dynamic system using a few input features. The resulting reduction in dimensionality can significantly improve computational efficiency and model training speed, making it advantageous for practical applications and large-scale structures. In addition, the method employed normalized modal parameters because normalization enhances the consistency and comparability of the input data across various structural conditions. By transforming raw modal parameters into a standardized format, the model becomes highly effective in capturing the structural variations.

In this paper, the first type of IF derives from calculating normalized natural frequencies. Multiple vibrational modes are employed to provide diverse information to the network, given that higher modes are more sensitive to damage. Each input factor j (IF_j) was computed through the value of each frequency j in the damaged condition (ω_{j_d}) and the respective frequency j in the healthy condition (ω_{j_h}), according to equation (2). However, the maximum number of vibrational modes in the input dataset depends on the conformity of the structure with the FE model and the performance of the system identification method.

$$\mathrm{IF}_j = \frac{\omega_{j_h} - \omega_{j_d}}{\omega_{j_h}}. \tag{2}$$

The second type of IF originates from normalized mode shapes, with the largest displacement value set to 1. This modal parameter provides spatial information about the structural system, leading to the adoption of only the first vibrational mode. Moreover, only the degrees of freedom referring to the predominant displacements of the structure were considered, as most of the structural information resides in these points.

The outputs were chosen to simulate the stiffness reduction caused by the damage in each element or region i of a structural system. Therefore, an output factor (OF_i) was arbitrated ranging from 0 to 1, where 1 signifies no damage, and 0 means that the element loses its stiffness completely. As the neural network model does not have a way to limit output values, depending on the dataset and the ANN training process and architecture, the stiffness reduction factor obtained for each element can be slightly less than zero or greater than one. In this way, a process of trial and error was executed pursuing the best hyperparameters related to network structure for each system.

Figure 2 exemplifies possible output factors obtained from different input factors. The system illustrated has three input factors (e.g., the first three natural frequencies) and five elements as output factors. There are two scenarios: (i) the healthy scenario and (ii) the damage scenario, where it is introduced 20% of stiffness reduction in element 4 ($\mathrm{OF}_4 = 0.8$).

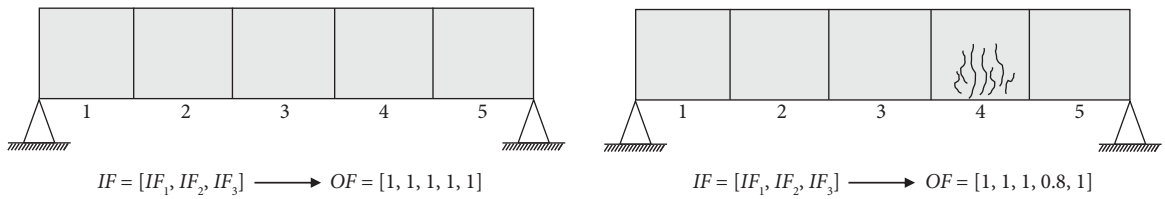

Figure 2: Examples of output factors for a healthy scenario and a damage scenario.

Among the existing network topologies, it was chosen to work with the feedforward network. In this type of neural network, the flow of information processing occurs only towards the outputs; that is, there is no return of signals to the previous layers. The networks were implemented through the feedforwardnet function of MATLAB [38]. The hyperparameters related to the training algorithm were fixed as 1000 epochs, 1×10^{-7} stopping criterion based on the MSE goal, 10 maximum validation failures, and 1×10^{-7} minimum performance gradient. In addition, the activation function for the hidden layers and the output layer were, respectively, hyperbolic tangent sigmoid transfer function and linear transfer function.

Figure 3 summarizes the framework for detecting damage in structures via ANNs. Initially, experimental and numerical responses to ambient excitation (acceleration signals) are used to identify the modal parameters through stochastic system identification, generating the numerical training data and experimental testing data. Next, the neural network is trained with the numerical dataset (input and output factors). Finally, the damage is detected, localized, and quantified with the experimental dataset.

3. Numerical Examples

To test the effectiveness of the damage detection method presented, experimental tests of a cantilever beam and a 10-bar plane truss were numerically simulated using matrix structural analysis. These structures were chosen to compare the results already obtained by other authors.

The ambient vibration was simulated by white Gaussian noise. Then, the system responses in accelerations were calculated by the Newmark method with an integration time-step of 0.005 s. The presence of noise in the signals to reproduce experimental conditions was also simulated by the white Gaussian noise. It was considered sensors placed at all the structure's vertical nodes because of the data availability. Finally, the data-driven stochastic subspace identification (SSI-DATA) technique (Peeters [39]) was implemented to obtain the modal parameters for the damage detection methods.

3.1. Cantilever Beam. The first system analyzed was a metallic cantilever beam 750 mm long with a square box cross-section with an external dimension of 25.4 mm and a wall thickness equal to 1 mm. The structure studied experimentally by Kaminski and Riera [40] was modeled with 25 Timoshenko beam elements, according to Figure 4. The specific weight, Young's modulus, Poisson's ratio, and Timoshenko shear factor are, respectively, 28 kN/m³, 68.6 GPa, 0.3, and 0.5. In addition, a concentrated mass of 18.2 g was added to all degrees of freedom to represent the presence of accelerometers in the experimental tests. To create the damping matrix, a damping ratio of 1% was considered in the first and fifth vibration modes.

As damage scenarios, the three cases studied by Zeni [41] were adopted: (1) element 20 with 20% stiffness reduction; (2) element 8 with 30% stiffness reduction; and (3) elements 5 and 12 with 50% and 30% stiffness reduction, respectively. The first two scenarios are present in Miguel et al. [15] and Fadel Miguel et al. [14]. The three studies mentioned used damage detection methods based on matrix updating using the backtracking search algorithm, harmony search algorithm, and hybrid Nelder–Mead algorithm, respectively.

The noise levels adopted in the acceleration signals were 3% and 5%. The respective natural frequencies obtained by the finite element model and through the stochastic system identification are in Tables 1 and 2.

The first two frequencies identified by the SSI-DATA method, in both noise situations, are close to the original values of the FE model. However, the value of the third frequency presents an error of around 10% because the system responses did not have enough contribution from the highest frequencies under the action of the white Gaussian noise. Therefore, damage detection was performed only with data from the first three vibration modes of the structure.

In training the neural networks, the first mode shape was used as input data, considering only the vertical degrees of freedom. As output data, the 25 elements of the system were adopted. The creation of the training set included single and multiple damage cases with two damaged elements. In these scenarios, the stiffness reduction variations in each element were from 10% to 60% in 10% intervals. Thus, a total of 1800 cases of multiple damage ($6 \times (25!/(2! \times 23!))$) and 150 cases of single damage (6×25) were obtained, totaling 1950 datasets.

After some tests of network architecture, it has opted for only one hidden layer with 25 neurons. The regression line is presented in Figure 5(a), comparing the model's predictions with the true labels of the dataset with a 10% tolerance limit of damage intensity, and Figure 5(b) indicates the mean squared error loss for the training and validation. Furthermore, Figures 6 and 7 show the results generated by the neural network for the three scenarios according to the applied noise levels.

The method efficiently identified and located the damage in the cantilever beam case. The quantification in the three scenarios was correct but with discrepancies up to 6.06%.

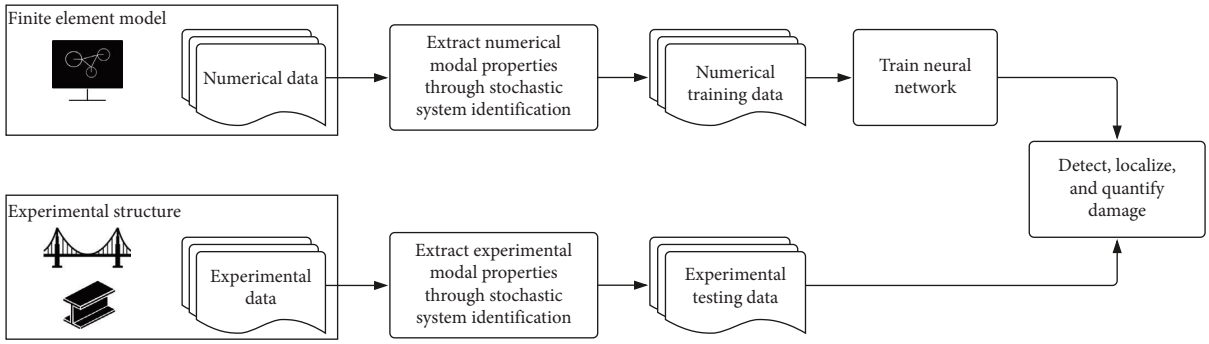

Figure 3: Damage detection method via ANN.

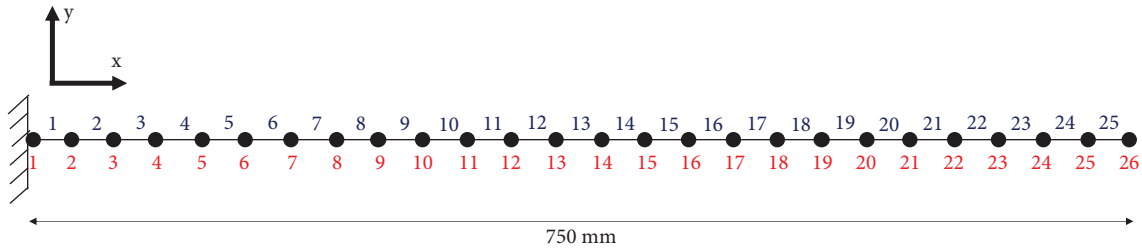

Figure 4: Beam modeled with 25 finite elements.

Table 1: Numerical natural frequencies of the cantilever beam (Hz).

Mode	*FE model*			
	Healthy scenario	Scenario 1	Scenario 2	Scenario 3
1	26.5600	26.5561	26.2459	25.3154
2	164.3250	163.8733	163.7602	161.3316
3	450.9722	447.0483	445.1953	446.4628

Table 2: Identified natural frequencies of the cantilever beam (Hz).

Mode	*SSI-DATA (3% noise)*				*SSI-DATA (5% noise)*			
	Healthy scenario	Scenario 1	Scenario 2	Scenario 3	Healthy scenario	Scenario 1	Scenario 2	Scenario 3
1	26.5657	26.5622	26.2662	25.3229	26.5657	26.5622	26.2662	25.3229
2	160.8429	160.4204	160.3151	157.9811	160.8425	160.4201	160.3148	157.9808
3	392.3989	389.7449	388.4807	389.3414	392.3984	389.7441	388.4799	389.3406

However, the damage values estimated by the ANNs were close to the exact values in both noise cases. The ANN had a similar performance in damage detection compared to the results presented by Zeni [41] and Miguel et al. [15] with methods based on matrix updating.

3.2. 10-Bar Plane Truss. The second structure analyzed was a 10-bar plane truss (Figure 8) studied by Begambre and Laier [42] and Fadel Miguel et al. [14]. All elements have a specific mass of 7700 kg/m^3, Young's modulus of 195 GPa, a moment of inertia of 3×10^{-8} m^4, and a cross-section of 4.2×10^{-4} m^2. The damping ratio was assumed to be 1% in the 1st and 3rd vibration modes.

To compare with the results obtained by Begambre and Laier [42] and Fadel Miguel et al. [14], the scenario of 15% stiffness reduction in bars 2 and 8 was analyzed. Both authors used a hybrid optimization approach: Begambre and Laier [42] used the PSO and Simplex algorithms, and Fadel Miguel et al. [14] employed a hybrid Nelder–Mead algorithm. Following these works, a noise of 3% was adopted in the acceleration signals of the healthy and damaged scenarios.

Table 3 presents the natural frequencies obtained by the finite element model and the stochastic system identification.

In the neural network training, the input data were the first mode shape (8 degrees of freedom), and the outputs were the structure bars. The training set was created from the FE model with single damage cases and multiple damage cases with two damaged elements. In these scenarios, the variations of stiffness reduction in each element were from 10% to 70% in 5% intervals. Thus, a total of 585 cases of multiple damage $(13 \times (10!/(2! \times 8!)))$ and 130 cases of

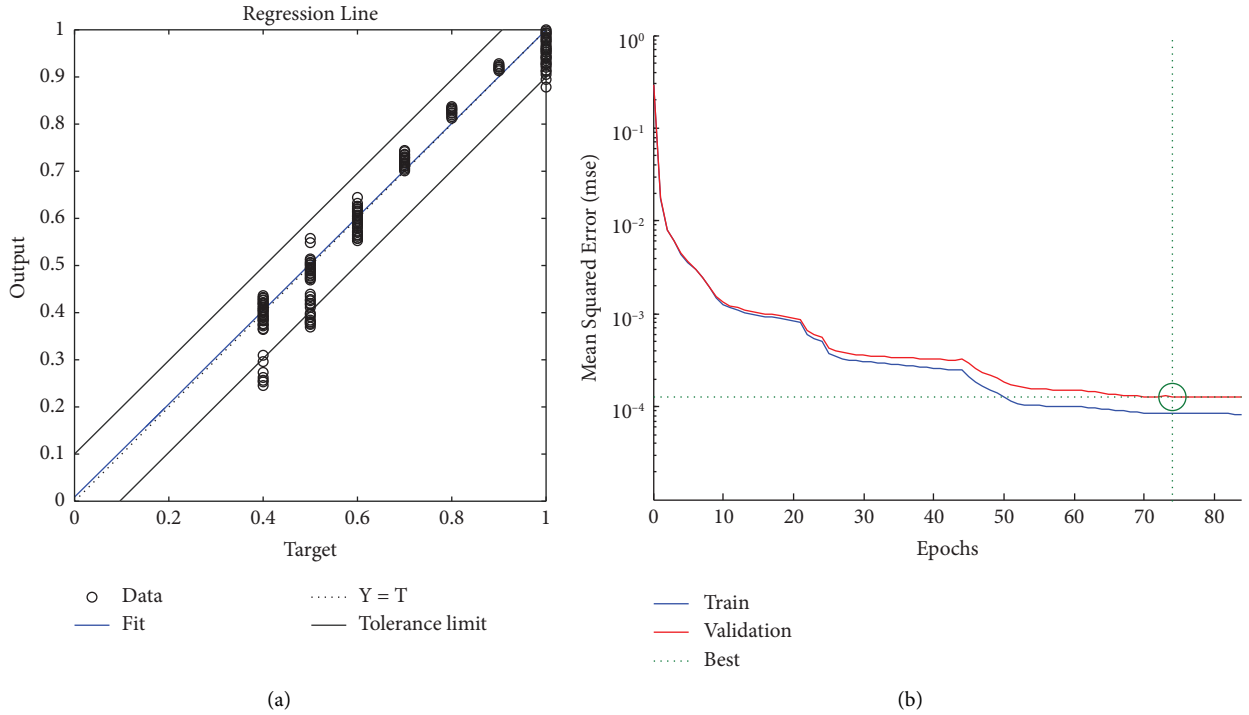

Figure 5: Numerical beam model: (a) regression line and (b) loss function.

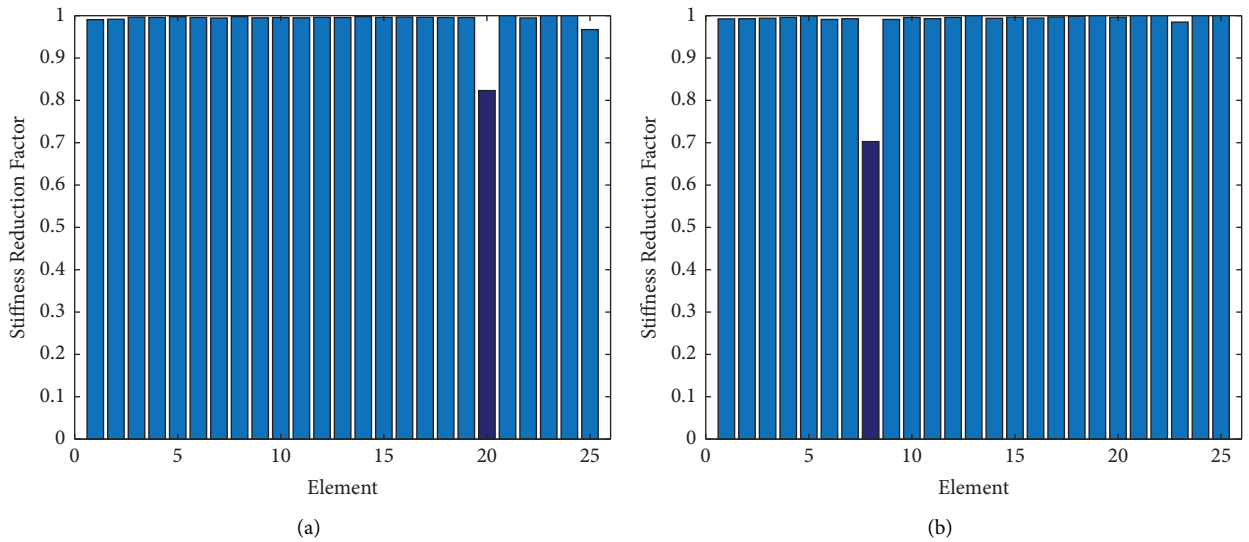

Figure 6: Continued.

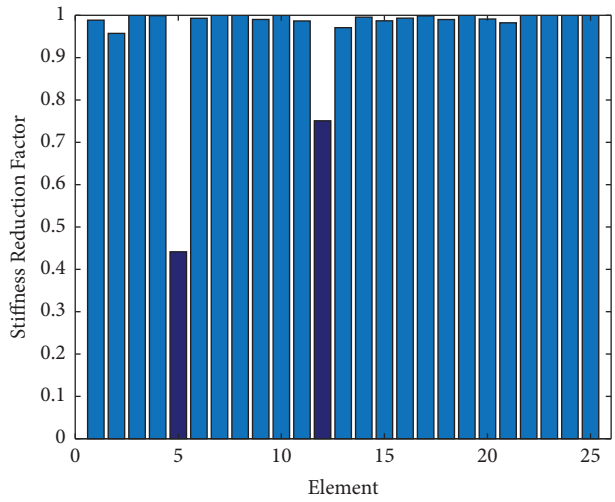

(c)

Figure 6: Numerical beam with 3% noise results: (a) damage scenario 1, (b) damage scenario 2, and (c) damage scenario 3.

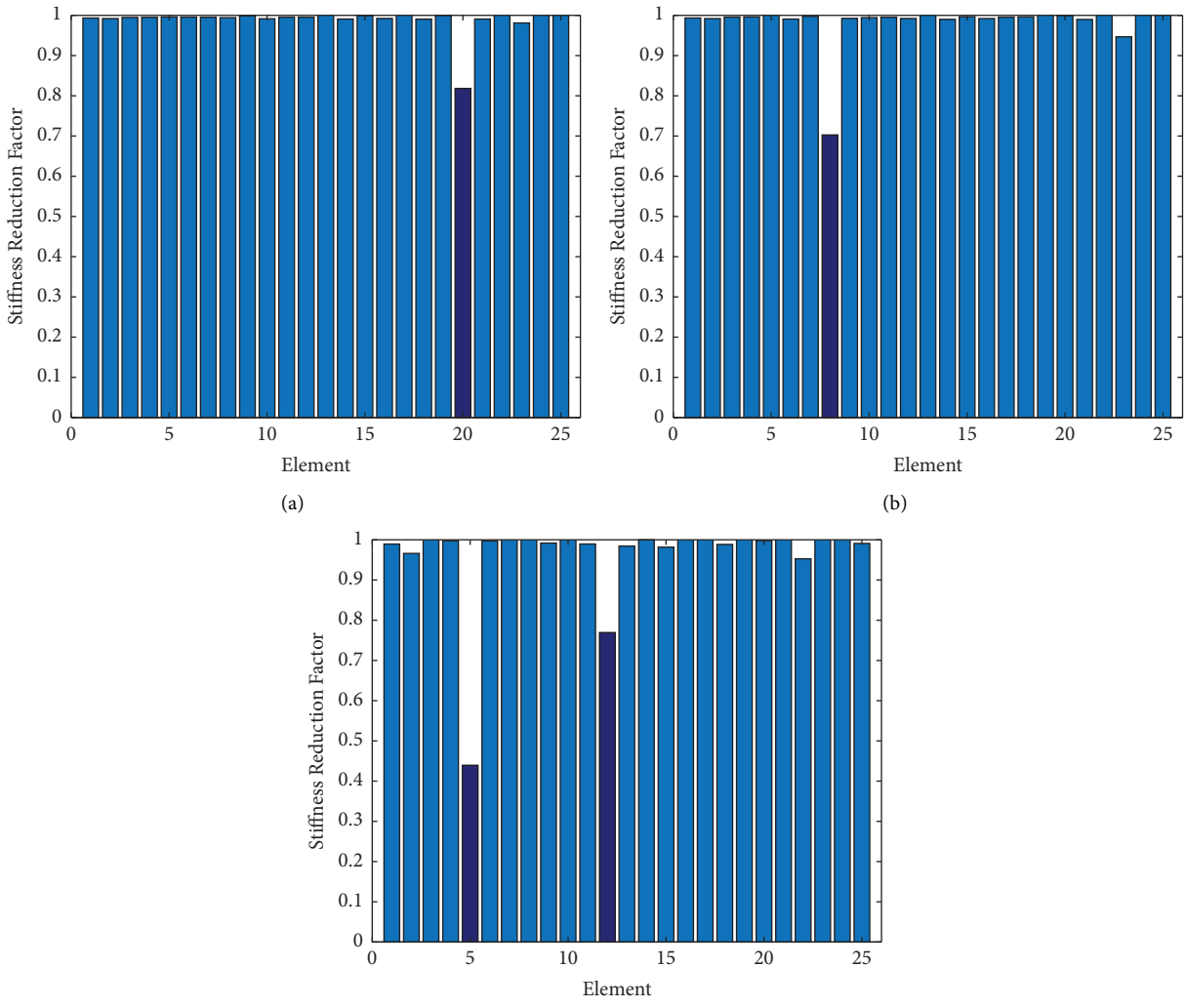

(a)

(b)

(c)

Figure 7: Numerical beam with 5% noise results: (a) damage scenario 1, (b) damage scenario 2, and (c) damage scenario 3.

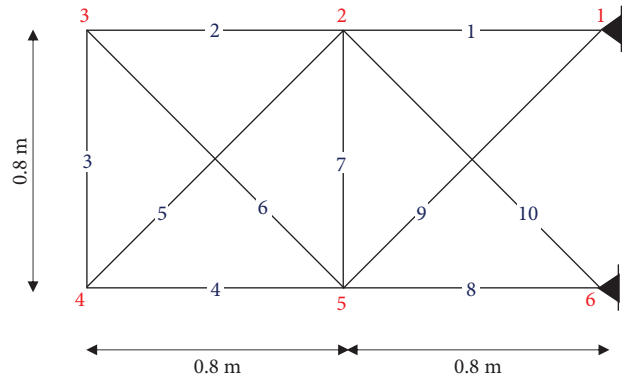

Figure 8: 10-bar truss structure.

Table 3: Natural frequencies of the 10-bar truss structure (Hz).

Mode	*FE model*		*SSI-DATA*	
	Healthy scenario	Damage scenario	Healthy scenario	Damage scenario
1	174.9996	170.5968	174.8116	170.4073
2	500.6687	484.7274	496.6709	480.9747
3	600.8525	593.0745	593.8417	586.3163

single damage (13×10) were obtained, totaling 715 datasets. The network architecture adopted was one hidden layer with 35 neurons. The mean square error of the model during training and the regression line are presented in Figure 9.

The results of the damage detection methodology are shown in Figure 10 and in Table 4 with the solutions obtained by Begambre and Laier [42] and Fadel Miguel et al. [14]. The framework used in this work correctly located and quantified the damage scenario.

4. Experimental System

The performance of the damage detection method was also verified in a system through experimental tests of a steel cantilever beam. The tests were carried out in the laboratory of the Applied Mechanics Group of the Federal University of Rio Grande do Sul (GMAP/UFRGS). The steel cantilever beam is 420 mm long, 39.5 mm wide, and 1.2 mm thick (Figure 11(a)). The specific mass, Young's modulus, Poisson's ratio, and Timoshenko shear factor of the beam are 8193.9 kg/m^3, 210 GPa, 0.3, and 0.5, respectively. This system was modeled with 28 Timoshenko beam elements (Figure 11(b)) using matrix structural analysis.

Lateral cuts were made in some of the beam elements to represent possible damage. The scenarios analyzed were as follows: (1) width reduction of element 13 to 33 mm; (2) width reduction of element 13 to 18.5 mm; and (3) width reduction of elements 8 and 13 to 17.5 mm and 18.5 mm, respectively. The experimental test was repeated at each progressive damage step.

4.1. Dynamic Tests. The dynamic tests were executed in the healthy condition for later comparison with the damage scenarios by means of accelerometers and the pulse 12 channel Brüel and Kjær type 3560 C acquisition system. As presented in Figure 12, the experimental tests were performed with three accelerometers, and Table 5 describes the properties of these devices. The sensor placement sought effective coverage of the experimental beam's modal parameters, especially the mode shapes. Therefore, a measurement point was required at the beam's free end (maximum displacement in the first mode shape) and two more measurement points were distributed equally in the beam's length.

To determine the modal parameters experimentally, small displacements were given at the beam, i.e., the system was in free vibration (Figure 13). At each stage, the dynamic tests were repeated to acquire the respective accelerograms.

4.2. System Identification. The three accelerograms obtained in each scenario were the input data for the SSI-DATA technique. The first five natural frequencies were accurately determined, as shown in Table 6. The highest difference found was 2.16% at the first natural frequency.

Figure 14 exhibits the mode shapes identified in the healthy scenario with the mode shapes of the numerical model. The fourth and fifth mode shapes could not be determined due to the lack of acquisition points because only three accelerometers were used. However, the first three modal shapes identified have 99.99% correlations with the numerical model, as shown by the modal assurance criterion (MAC) (Abdel Wahab and De Roeck [6]) in Figure 15.

4.3. Damage Detection. In the damage detection method based on neural networks for the case of the steel beam, the input data were the first five natural frequencies, and the outputs were the system's 28 elements. The training data

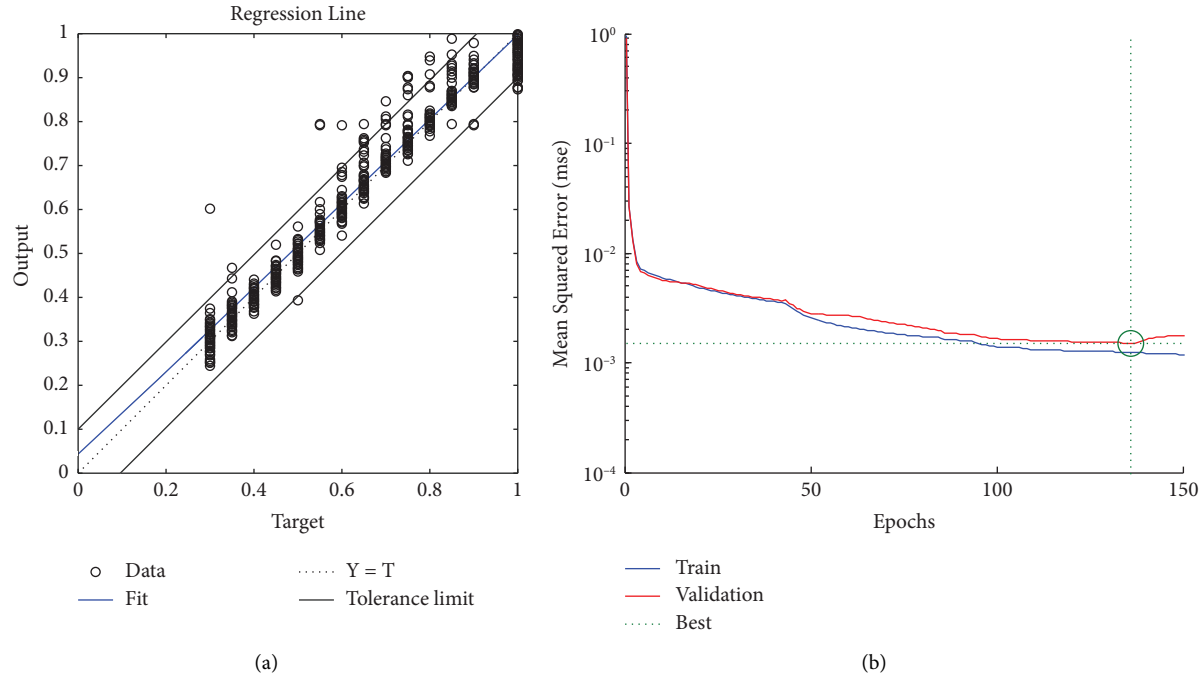

Figure 9: Numerical 10-bar truss model: (a) regression line and (b) loss function.

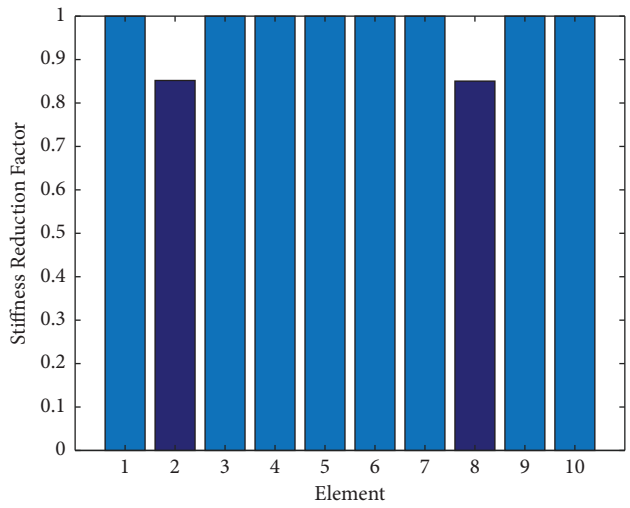

Figure 10: 10-bar truss structure result.

included only single damage cases from the FE model. In these scenarios, the variations of stiffness reduction in each element were from 5% to 60% in 5% intervals, totaling 336 datasets (12×28). After some tests of variations in the network architecture, three hidden layers with 5, 14, and 25 components were chosen. The mean square error of the model during training and the regression line are presented in Figure 16.

Figure 17 shows the results generated by the ANN for the three analyzed scenarios. The proposed method presented effective damage localization results in the experimental tests, successfully identifying the damaged elements in all cases. In damage scenario 3, element 7 also displayed a fault state, possibly due to its proximity to the damaged region.

Table 4: Results of the damage detection for the 10-bar truss structure.

Bar	Exact damage	*Predicted damage*		
		Begambre and Laier [42]	Fadel Miguel et al. [14]	ANN
1	1	1	0.9995	0.9974
2	**0.85**	**0.8476**	**0.8537**	**0.8544**
3	1	0.9987	1	1.0447
4	1	0.9862	0.9998	1.0087
5	1	0.9829	0.9946	1.0115
6	1	0.9992	1	1
7	1	1	1	1.0165
8	**0.85**	**0.8503**	**0.8500**	**0.8460**
9	1	0.9996	1	0.9977
10	1	1	1	1.0094

Bold highlights elements that have been damaged.

The quantification results for damage detection showed some inaccuracies. However, the training did not include multiple damage cases because a larger database was impairing the network learning process, consequently affecting the generated results.

5. Z24 Bridge

Finally, the proposed damage detection method was applied and verified on a real civil structure used as a benchmark in the scientific community, the Z24 bridge (Switzerland). In this work, a multiple damage case caused by the settlement of one of the system's piers was analyzed.

The Z24 bridge was selected by the Brite–Euram research project BE-3175, SIMCES (System Identification to Monitor Civil Engineering Structures), as a study object to develop a methodology for structural integrity monitoring. The work

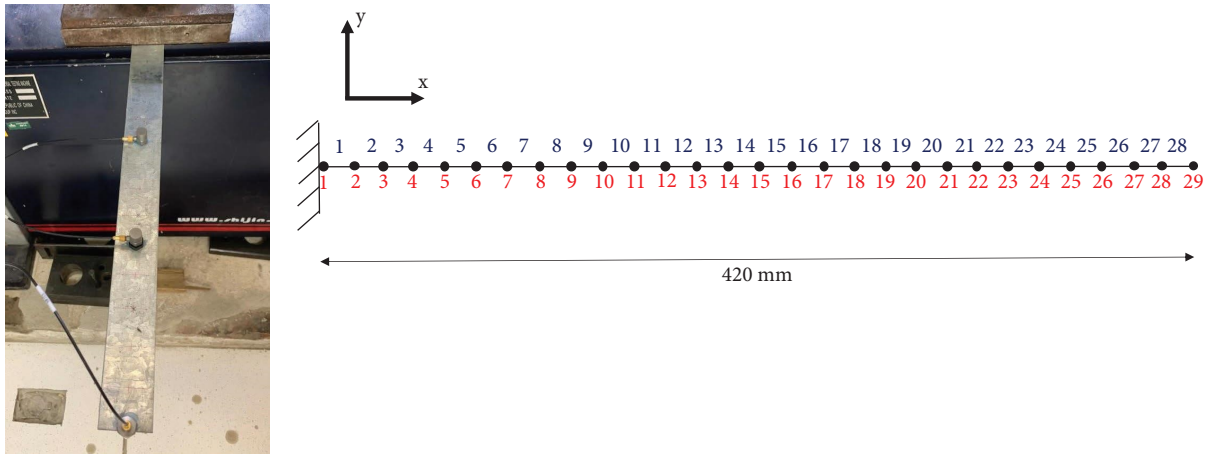

(a) (b)

Figure 11: Experimental steel beam: (a) instrumented with accelerometers and (b) discretized.

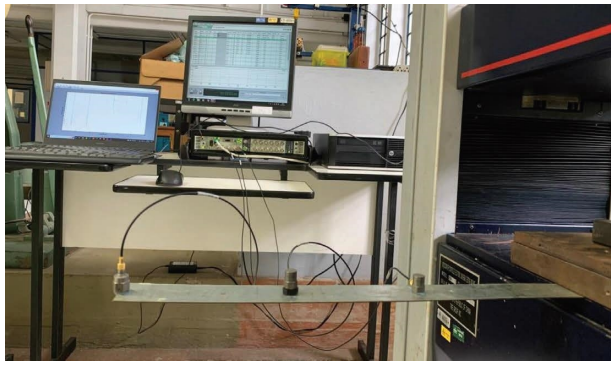

Figure 12: Experimental beam and acquisition system.

Table 5: Accelerometers properties.

Position	Manufacturer	Model	Serial number	Mass (g)
Node 11	PCB piezotronics	352C33	86702	5.631
Node 19	PCB piezotronics	352C33	86703	7.949
Node 29	Brüel & Kjær	4514B 4x	51467x	8.723

coordinated by the Catholic University of Leuven (Department of Civil Engineering, Structural Mechanics Section) included monitoring the structure for one year and performing progressive damage tests before the demolition of the bridge in 1998 (Roeck [43]).

This structure was in the Canton of Bern in Switzerland, connecting Koppigen and Utzenstorf, and overpassed Highway A1, which connected the cities of Bern and Zurich. The bridge had three spans and two lanes and was about 60 m long (Figure 18). The two central piers were clamped into the girders, while the two triplets of columns at both ends supported the bridge at the endpoints. All supports were rotated regarding the longitudinal axis of the structure forming a slightly skew bridge (Peeters and De Roeck [44]). The girder was a two-box cell with posttensioned concrete (Figure 19).

In total, 17 progressive damage tests (PDTs) were performed, which are described in detail by Krämer [45], Maeck and De Roeck [46], and Reynders and De Roeck [47]. The PDTs were selected according to the occurrence frequency, based on the number of citations in the literature and the experience of Swiss bridge owners (Roeck [43]). The first set of PDTs considered the foundation settlement of the Koppigen pier. The settlement scenarios were simulated by lowering the pier ($x = 44$ m), which caused several cracks in the girder, as illustrated in Figure 20. Other failure modes of bridge piers and their impact on structures are presented by Govahi et al. [48] and Liu et al. [49], for instance.

In this work, PDT 2 was adopted as the healthy scenario, and the 95 mm settlement of the column (PDT 6) as the damaged scenario.

5.1. System Identification. The modal parameters of the Z24 bridge were identified from the data of the ambient vibration tests, which included nine setups of 15 accelerometers on the deck (2 triaxial, 3 biaxial, and 10 uniaxial), 2 triaxial accelerometers on one of the piers, and 3 reference accelerometers (1 triaxial and 2 uniaxial), totaling 33 records. The sampling frequency and acquisition time were 100 Hz and 655.36 s, respectively. Table 7 presents the identified natural frequencies by the SSI-DATA technique for the healthy and damaged scenarios.

5.2. Finite Element Model Updating. Teughels and De Roeck [50] and Reynders et al. [51] developed the FE model used in this work employing ANSYS APDL [52] with beam elements (BEAM4 and BEAM 44, 6 degrees of freedom per node). The authors modeled the girder with 82 beam elements and the piers, columns, and abutments with 44 beam elements, according to Figure 21. Mass elements were added to represent the cross girders and foundations, considering concentrated translational mass and rotary inertial components.

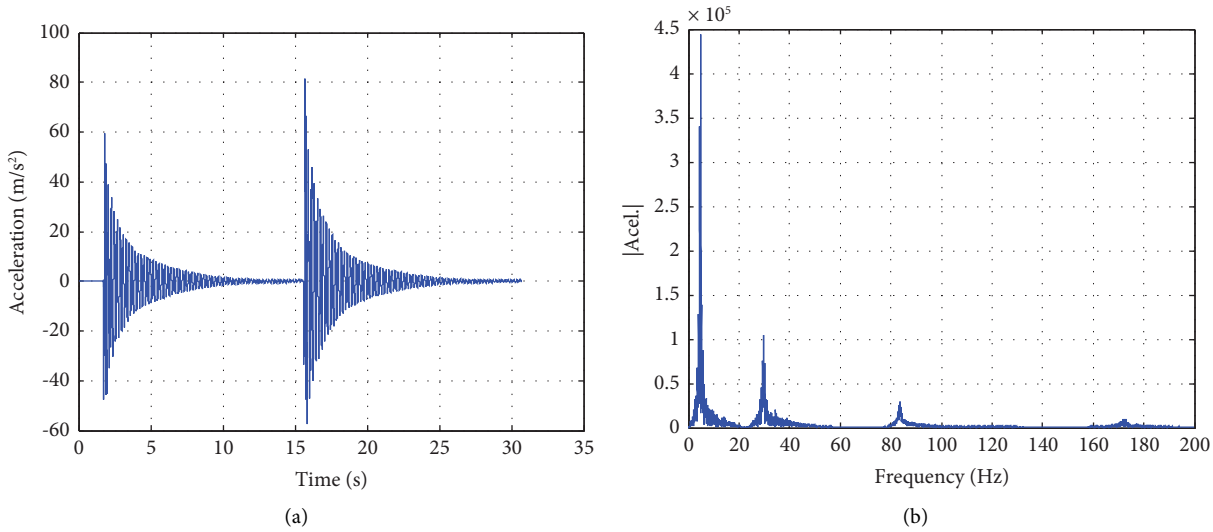

Figure 13: Node 29 (healthy scenario) of the experimental beam: (a) accelerogram, (b) FFT.

Table 6: Natural frequencies of the experimental beam (Hz).

Mode	FE model	*SSI-DATA*			
	Healthy scenario	Healthy scenario	Scenario 1	Scenario 2	Scenario 3
1	4.9341	4.8270	4.8137	4.7989	4.6853
2	30.5389	29.9510	29.9172	29.5635	29.4792
3	85.6315	85.4507	84.8619	84.7127	83.4732
4	178.8478	177.6512	176.5049	175.2284	171.8705
5	281.9240	277.3123	275.5140	275.4523	273.9630

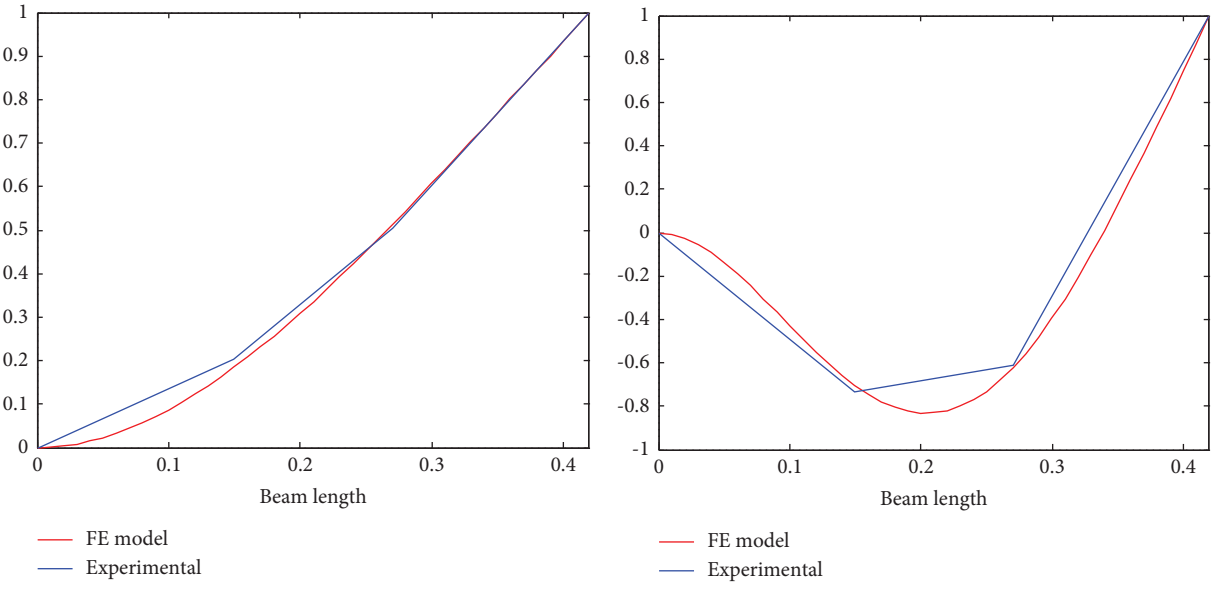

Figure 14: Continued.

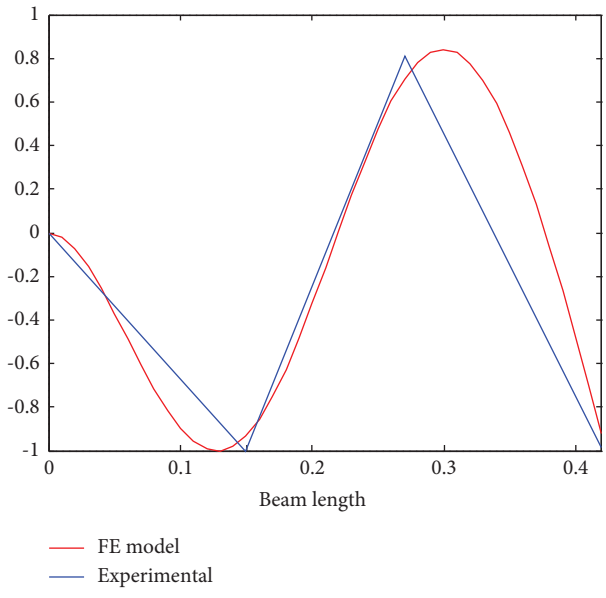

(c)

Figure 14: Experimental and numerical mode shapes: (a) mode 1, (b) mode 2, and (c) mode 3.

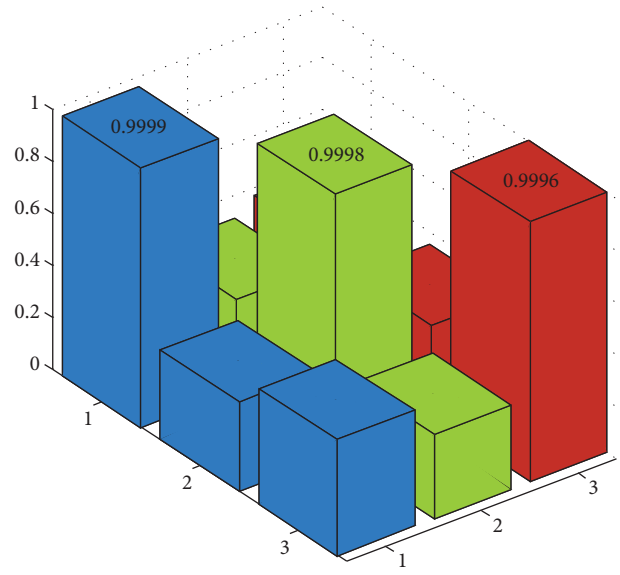

Figure 15: MAC of experimental and numerical mode shapes in the healthy scenario.

Initially, Young's modulus $E_0 = 37.5$ GPa and shear modulus $G_0 = 20$ GPa were considered. To account for the influence of the soil on the system, spring elements were included around the pillars and at the base of the abutments. The soil stiffness parameters adopted for the springs were $K_{y,p} = 180 \times 10^6$ N/m³ and $K_{h,p} = 210 \times 10^6$ N/m³ (under the piers, at $(x) = 14$ and 44 m); $K_{v,c} = K_{h,c} = 100 \times 10^6$ N/m³ (under the columns, at $(x) = 0$ and 58 m); $K_{v,a} = 180 \times 10^6$ N/m³ and $K_{h,a} = 200 \times 10^6$ N/m³ (at the abutments); $K_{v,ac} = K_{h,ac} = 100 \times 10^6$ N/m³ (around the columns).

This numerical model had the values of Young's modulus and shear modulus of the bridge girder and soil stiffness parameters updated according to the six natural frequencies identified in the healthy scenario presented in Table 7. This was carried out through a minimization problem using the objective function:

$$\prod(\varnothing) = \sum_{j=1}^{\mathrm{Nm}} \frac{1}{2} \left(\frac{\omega_j^{2(\varnothing)} - \widetilde{\omega}_j^2}{\widetilde{\omega}_j^2} \right)^2, \tag{3}$$

where $\widetilde{\omega}_j$ is the identified natural frequency of the jth mode and ω_j is the natural frequency j of the numerical model as a function of the variable $\varnothing$. In this process, 36 variables were updated: 17 Young's moduli and 17 shear moduli, with the moduli of intermediate elements interpolated from the main elements; the vertical soil stiffness under the piers $K_{v,p}$ and the horizontal stiffness under the abutments $K_{h,a}$.

The difference between the first six experimental frequencies and the updated numerical frequencies was less than 1%, as shown in Table 8. The updated soil stiffness parameters were $K_{v,p} = 147.5 \times 10^6$ N/m³ and $K_{h,a} = 146.4 \times 10^6$ N/m³, and the updated bending stiffness (EIy) and torsional stiffness (GIx) parameters in comparison with initial model values are presented in Figure 22.

5.3. Damage Detection. Nine regions of the bridge girder were established (Figure 23) in the updated FE model, aiming to reduce the stiffness reduction factors in the damage detection method. The regions were defined to represent the areas of influence of the piers and abutments in addition to girder partitions.

The damage detection method used the first six natural frequencies as input data and the girder regions as outputs. The training data included single damage cases of the finite element model. In these scenarios, the stiffness reduction variations in each region ranged from 5% to 80% in 5% intervals, totaling 144 datasets (16×9). After some

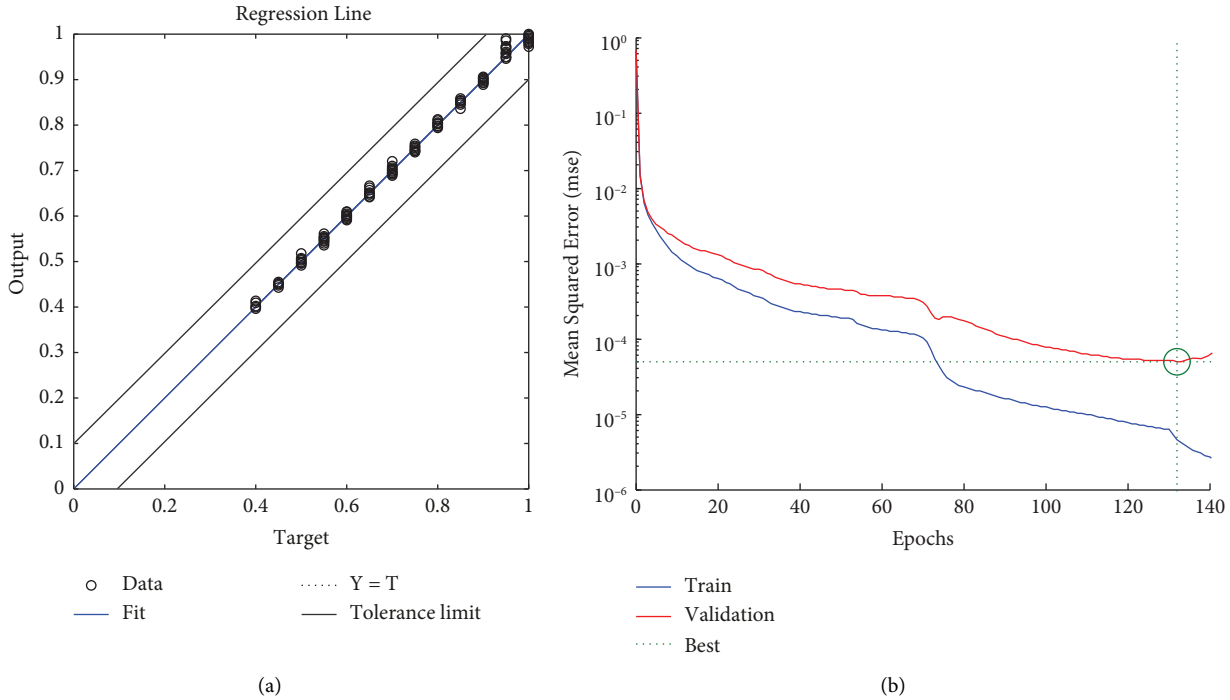

Figure 16: Experimental beam model: (a) regression line and (b) loss function.

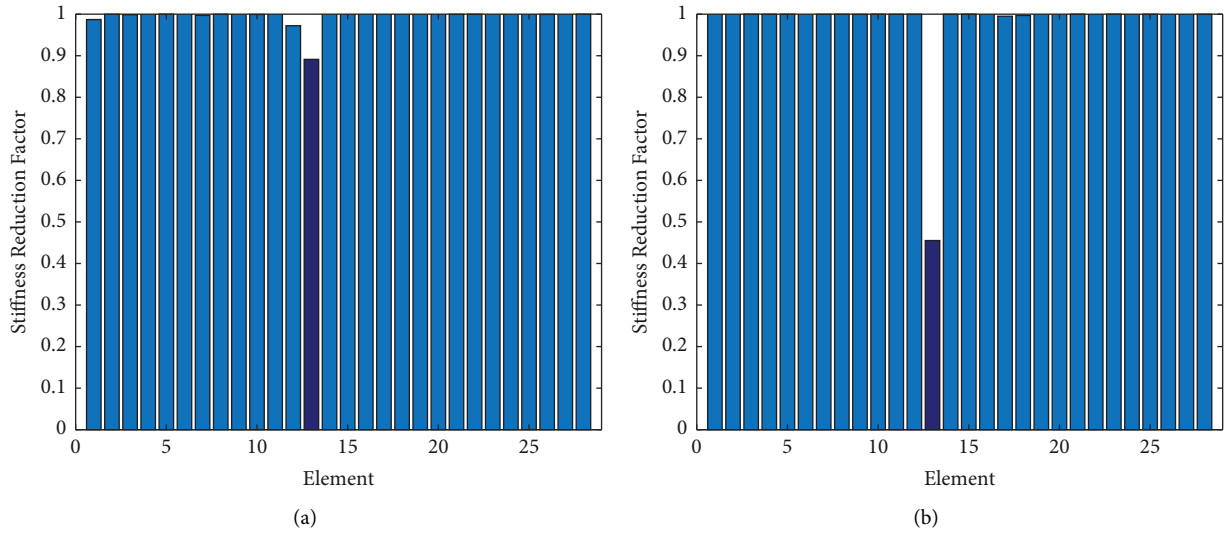

Figure 17: Continued.

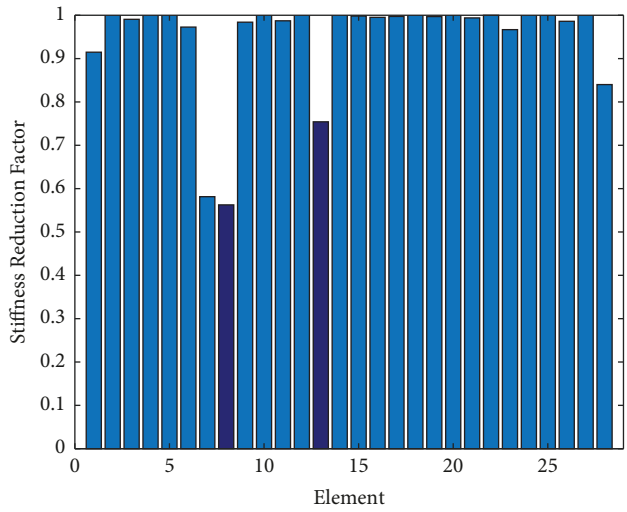

(c)

Figure 17: Experimental beam results: (a) damage scenario 1, (b) damage scenario 2, and (c) damage scenario 3.

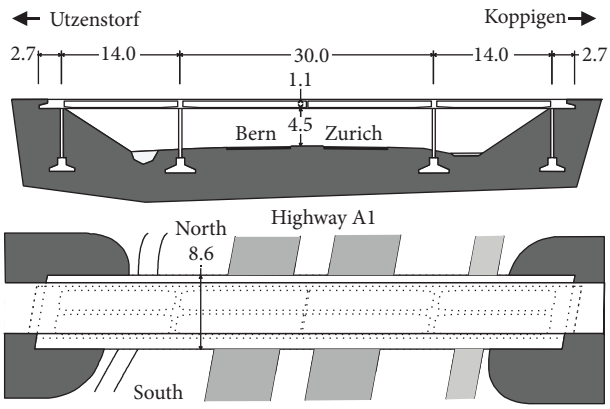

Figure 18: Z24 bridge: longitudinal section and plan view.

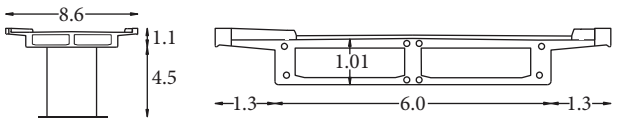

Figure 19: Z24 bridge: cross-section.

architecture tests, it was decided to add the numerical and experimental frequency values of the healthy scenario to the training data. Three hidden layers with 5, 18, and 9 neurons were used. The mean square error of the model during training and the regression line are presented in Figure 24. The network solution (output factors) is presented in Figure 25.

In the case of the Z24 bridge, the damage detection method was able to locate the main damaged region (region 7), where the pier settlement and the cracks in the adjacent regions of the girder occurred. Secondary damage regions from cracking in neighboring areas of the pier (regions 6 and 8) were not as easily located, with only region 6 identified. It was not possible to verify the damage levels identified because there was no real quantitative response.

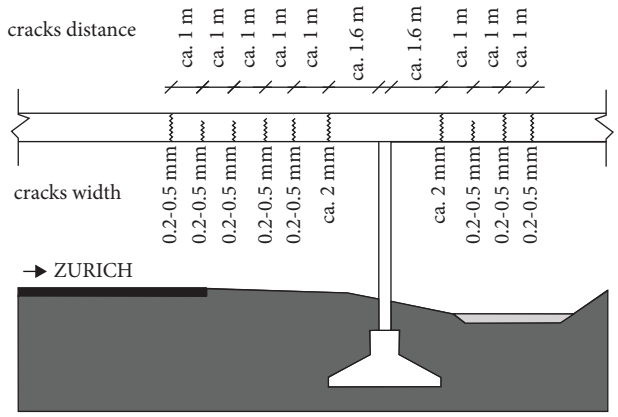

Figure 20: Cracks in the bridge girder after lowering the pier at 44 m.

Table 7: Identified natural frequencies of the Z24 bridge.

	SSI-DATA		
Mode	Healthy scenario (Hz)	Damage scenario (Hz)	Difference (%)
1	3.87	3.66	5.65
2	5.01	4.92	1.73
3	9.79	9.24	5.56
4	10.31	9.68	6.09
5	12.79	12.15	4.99
6	13.50	13.44	0.44
		Mean	4.08

The results showcased in Figure 25 for damage detection and localization demonstrate a superior performance on a global level compared to prior studies. For instance, in the work by Sony et al. [53], the absence of quantitative information related to physics properties within the damage index hindered the ability to infer damage without undertaking a global analysis of each structural component

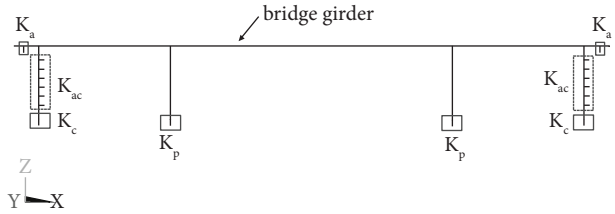

Figure 21: FE model of the Z24 bridge.

Table 8: Updated numerical frequencies of the Z24 bridge.

Vibration mode	*FE model*		SSI-DATA (Hz)	Difference (%)
	Initial (Hz)	Updated (Hz)		
1	3.73	3.86	3.87	−0.26
2	5.14	5.04	5.01	0.70
3	9.64	9.75	9.79	−0.33
4	10.25	10.37	10.31	0.52
5	12.52	12.81	12.79	0.14
6	13.35	13.39	13.50	−0.85

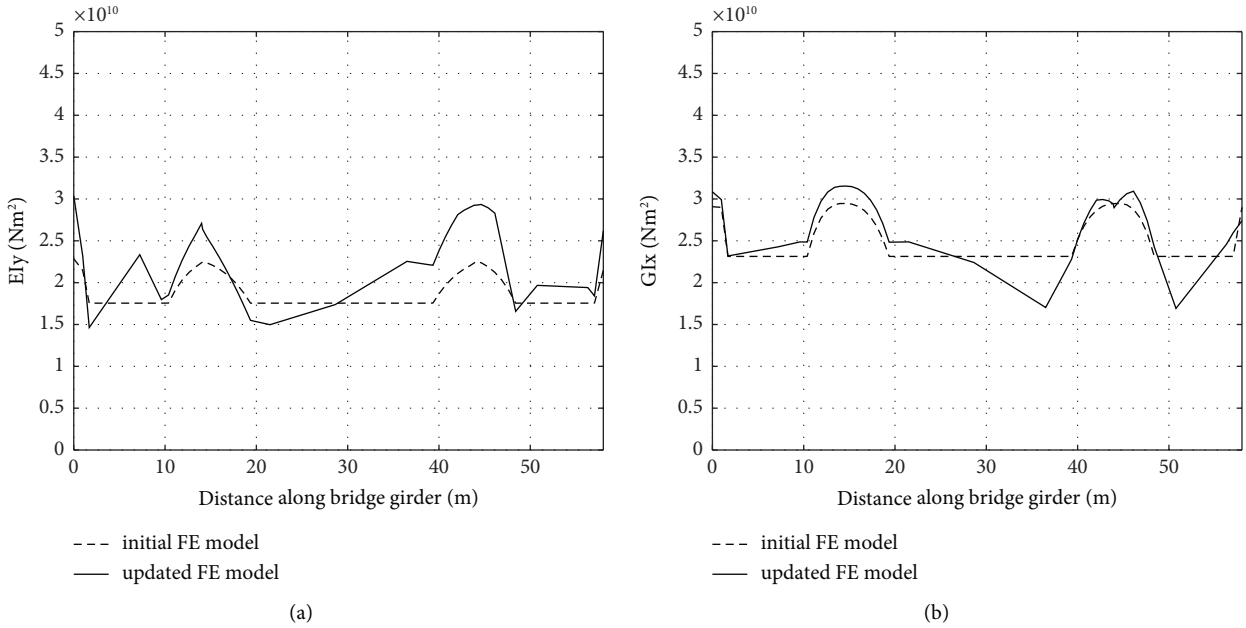

Figure 22: Updating results: (a) bending stiffness distribution and (b) torsional stiffness distribution.

across various damage scenarios. Furthermore, in the work by Masciotta et al. [54], satisfactory results were obtained when employing five points within the spectral damage localization index. These points are equivalent to specific regions of the bridge, which was nearly half of what was implemented in this paper.

It must be emphasized that the neural network needs data from the same domain in the training and test dataset to achieve the necessary accuracy. This work used model updating to align the numerical domain and the experimental domain. This process fine-tunes the numerical model using experimental data to reduce their discrepancy. Another approach to address the divergence between different domains is data preprocessing. The effects of mismatched modal parameters can be minimized by aligning the statistical properties of different datasets, such as mean, variance, and distribution. Alternatively, domain adaptation techniques, a subcategory of transfer learning, can be employed. This approach enables the model to generalize from one domain to another (e.g., numerical simulations to experimental systems) by learning their differences and similarities. This can reduce the strict requirement for domain alignment and alleviate computational problems in large-scale structures.

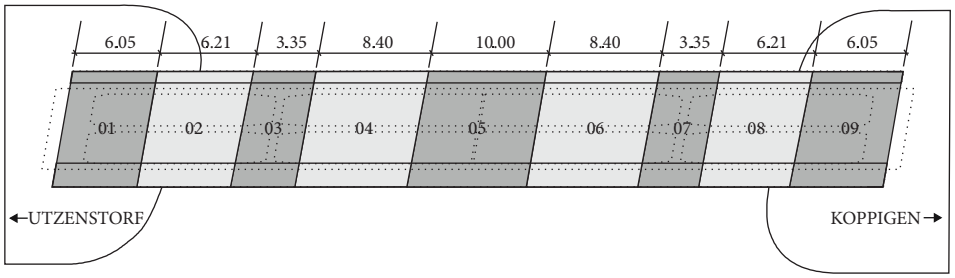

Figure 23: Regions of the Z24 bridge for damage detection.

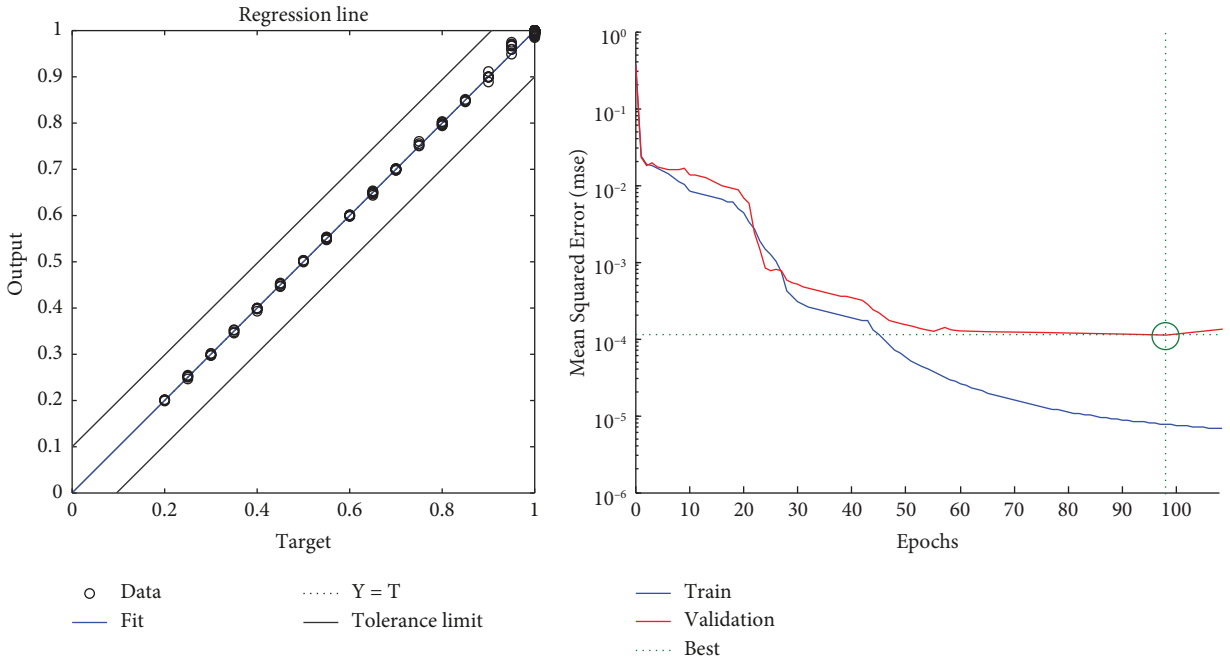

Figure 24: Z24 bridge model: (a) regression line and (b) loss function.

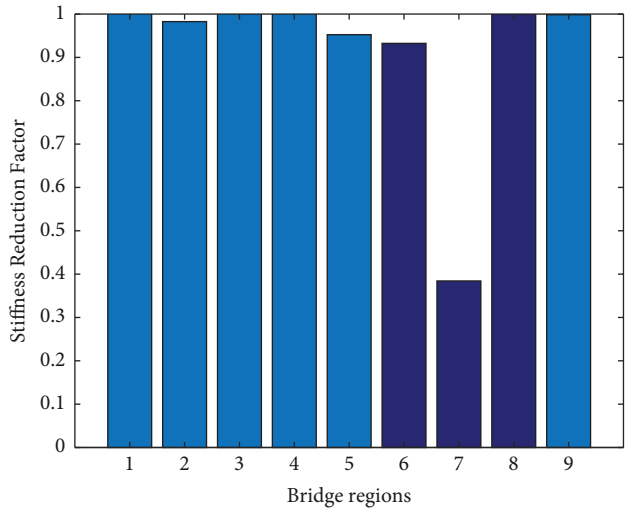

Figure 25: Damage detection of the Z24 bridge.

6. Conclusions

This paper presented a method for damage detection via artificial neural networks in a single stage using numerical training data. The methodology was applied, compared, and evaluated through numerical simulations (cantilever beam and 10-bar truss) and experimental tests (steel beam and Z24 bridge). In this way, it was possible to evaluate the method's performance to identify, locate, and quantify the scenarios of single and multiple damages. The results obtained allow drawing the following conclusions:

(1) The ANNs showed promising results in locating and quantifying damage and can be used for practical purposes. In the simulation cases, the method presented similar results to those found by other authors in the literature who used damage detection methods based on matrix updating. Moreover, even with noise in the acceleration signals and changes in the first vibration mode of 0.015% (cantilever beam case), the framework could perform the three damage tasks satisfactorily.

(2) In the experimental lab structure, the methodology proved to be effective in detecting, locating, and quantifying single and multiple damage scenarios with a mean difference of 0.47% and 2.26% between the frequencies in the healthy and damaged conditions, respectively.

(3) In the study of the Z24 bridge, it was possible to verify the method's effectiveness in detecting and locating damage, proving that the methodology can be used in real civil structures. Additionally, even with an evaluation based only on natural frequencies, the method could estimate the damage caused by the pier settlement, despite a mean difference of 4.08% between the frequencies in the healthy and damaged conditions.

Future work can be carried out investigating ill-conditioning problems that can happen with larger numbers of elements as output factors. As was observed in the Z24 bridge, adopting a few input factors required fewer regions as outputs. Therefore, structures modeled with more elements should be investigated with a different approach. Furthermore, the framework should be extended to accommodate environmental and operational conditions, such as temperature variations and include transfer learning to avoid problems related to mismatched modal parameters.

Data Availability

All data, models, or codes that support the findings of this study are available from the corresponding author upon reasonable request.

Disclosure

An earlier version of this paper was presented in Portuguese as a master's dissertation [17] at the Federal University of Rio Grande do Sul.

Conflicts of Interest

The authors declare that they have no conflicts of interest.

Acknowledgments

The authors acknowledge the financial support of Conselho Nacional de Desenvolvimento Científico e Tecnológico (CNPq) and Coordenação de Aperfeiçoamento de Pessoal de Nível Superior (CAPES), Brazil, and the KU Leuven Structural Mechanics Section as the source of the Z24 bridge data.

References

[1] W. X. Ren, Y. Q. Lin, and S. E. Fang, "Structural damage detection based on stochastic subspace identification and statistical pattern recognition: I. Theory," *Smart Materials and Structures*, vol. 20, no. 11, Article ID 115009, 2011.

[2] O. S. Salawu, "Detection of structural damage through changes in frequency a review," *Engineering Structures*, vol. 19, no. 9, pp. 718–723, 1997.

[3] R. J. Allemang and D. L. Brown, "A correlation coefficient for modal vector analysis," in *Proceedings of the 1st International Modal Analysis Conference*, IMAC, Orlando, FL, USA, November, 1982.

[4] R. O. Curadelli, J. D. Riera, D. Ambrosini, and M. G. Amani, "Damage detection by means of structural damping identification," *Engineering Structures*, vol. 30, no. 12, pp. 3497–3504, 2008.

[5] A. K. Pandey, M. Biswas, and M. M. Samman, "Damage detection from changes in curvature mode shapes," *Journal of Sound and Vibration*, vol. 145, no. 2, pp. 321–332, 1991.

[6] M. M. Abdel Wahab and G. De Roeck, "Damage detection in bridges using modal curvatures: application to a real damage scenario," *Journal of Sound and Vibration*, vol. 226, no. 2, pp. 217–235, 1999.

[7] P. Cornwell, S. W. Doebling, and C. R. Farrar, "Application of the strain energy damage detection method to plate-like structures," *Journal of Sound and Vibration*, vol. 224, no. 2, pp. 359–374, 1999.

[8] D. Bernal, "Load vectors for damage localization," *Journal of Engineering Mechanics*, vol. 128, no. 1, pp. 7–14, 2002.

[9] L. F. F. Miguel, L. F. F. Miguel, J. D. Riera, and R. C. R. D. Menezes, "Damage detection in truss structures using a flexibility based approach with noise influence consideration," *Structural Engineering and Mechanics*, vol. 27, no. 5, pp. 625–638, 2007.

[10] H. Sohn and K. H. Law, "A bayesian probabilistic approach for structure damage detection," *Earthquake Engineering and Structural Dynamics*, vol. 26, no. 12, pp. 1259–1281, 1997.

[11] W. Zheng, J. Shen, and J. Wang, "Improved computational framework for efficient bayesian probabilistic inference of damage in truss structures based on vibration measurements," *Transportation Research Record*, vol. 2460, no. 1, pp. 117–127, 2014.

[12] K. M. Liew and Q. Wang, "Application of wavelet theory for crack identification in structures," *Journal of Engineering Mechanics*, vol. 124, no. 2, pp. 152–157, 1998.

[13] H. Altammar, A. Dhingra, and S. Kaul, "Use of wavelets for mixed-mode damage diagnostics in warren truss structures," in *Proceedings of the ASME 2014 International Design Engineering Technical Conferences and Computers and*

Information in Engineering Conference, IDETC/CIE, New York, NY, USA, August, 2014.

[14] L. F. Fadel Miguel, R. Holdorf Lopez, and L. F. Fadel Miguel, "A hybrid approach for damage detection of structures under operational conditions," *Journal of Sound and Vibration*, vol. 332, no. 18, pp. 4241–4260, 2013.

[15] L. F. F. Miguel, L. F. F. Miguel, J. Kaminski Jr., and J. D. Riera, "Damage detection under ambient vibration by harmony search algorithm," *Expert Systems with Applications*, vol. 39, no. 10, pp. 9704–9714, 2012.

[16] L. F. F. Miguel, L. F. F. Miguel, and J. K. Jr, "Stochastic system identification and damage detection using firefly algorithm," *International Journal of Lifecycle Performance Engineering*, vol. 1, no. 4, pp. 357–379, 2014.

[17] D. K. Monteiro, "Detection, localization, and quantification of damage in structures via metaheuristic algorithms and artificial neural networks," Master dissertation – Programa de Pós-Graduação em Engenharia Civil, Universidade Federal do Rio Grande do Sul, PPGEC/UFRGS, Porto Alegre, Brazil, 2023.

[18] X. Wu, J. Ghaboussi, and J. H. Garrett Jr., "Use of neural networks in detection of structural damage," *Computers and Structures*, vol. 42, no. 4, pp. 649–659, 1992.

[19] M. Mehrjoo, N. Khaji, H. Moharrami, and A. Bahreininejad, "Damage detection of truss bridge joints using Artificial Neural Networks," *Expert Systems with Applications*, vol. 35, no. 3, pp. 1122–1131, 2008.

[20] V. Srinivas, K. Ramanjaneyulu, and C. A. Jeyasehar, "Multi-stage approach for structural damage identification using modal strain energy and evolutionary optimization techniques," *Structural Health Monitoring*, vol. 10, no. 2, pp. 219–230, 2010.

[21] H. W. Shih, D. P. Thambiratnam, and T. H. T. Chan, "Damage detection in truss bridges using vibration based multi-criteria approach," *Structural Engineering and Mechanics*, vol. 39, no. 2, pp. 187–206, 2011.

[22] A. Garcia-Perez, J. P. Amezquita-Sanchez, A. Dominguez-Gonzalez, R. Sedaghati, R. Osornio-Rios, and R. J. Romero-Troncoso, "Fused empirical mode decomposition and wavelets for locating combined damage in a truss-type structure through vibration analysis," *Journal of Zhejiang University- Science*, vol. 14, no. 9, pp. 615–630, 2013.

[23] H. Tran-Ngoc, S. Khatir, G. De Roeck, T. Bui-Tien, and M. Abdel Wahab, "An efficient artificial neural network for damage detection in bridges and beam-like structures by improving training parameters using cuckoo search algorithm," *Engineering Structures*, vol. 199, Article ID 109637, 2019.

[24] S. W. Doebling, C. R. Farrar, M. E. Prime, and D. W. Shevitz, "Damage identification and health monitoring of structural and mechanical systems from changes in their vibration characteristics: a literature review," Los Alamos Laboratory Report LA-13070-MS, 1996.

[25] W. Fan and P. Qiao, "Vibration-based damage identification methods: a review and comparative study," *Structural Health Monitoring*, vol. 10, no. 1, pp. 83–111, 2011.

[26] Y. An, E. Chatzi, S.-H. Sim, S. Laflamme, B. Blachowski, and J. Ou, "Recent progress and future trends on damage identification methods for bridge structures," *Structural Control and Health Monitoring*, vol. 26, no. 10, p. e2416, 2019.

[27] J. D. Villalba and J. E. Laier, "Detección de Daño Estructural Utilizando Redes Neuronales Artificiales: un estado del Arte," *Cadernos de Engenharia de Estruturas*, vol. 17, no. 67, pp. 1–19, 2017.

[28] M. Salkhordeh, M. Mirtaheri, N. Rabiee, E. Govahi, and S. Soroushian, "A rapid machine learning-based damage detection technique for detecting local damages in reinforced concrete bridges," *Journal of Earthquake Engineering*, vol. 27, pp. 1–34, 2023.

[29] G. Mariniello, T. Pastore, C. Menna, P. Festa, and D. Asprone, "Structural damage detection and localization using decision tree ensemble and vibration data," *Computer-Aided Civil and Infrastructure Engineering*, vol. 36, no. 9, pp. 1129–1149, 2020.

[30] C. R. Farrar and K. Worden, *Structural Health Monitoring: A Machine Learning Perspective*, John Wiley & Sons, Hoboken, NJ, USA, 2012.

[31] A. Rytter, *Vibrational based inspection of civil engineering structures*, Ph.D. Dissertation, Department of Building Technology and Structural Engineering, Aalborg University, Aalborg, Denmark, 1993.

[32] S. P. Hekmati Athar, M. Taheri, J. Secrist, and H. Taheri, "Neural network for structural health monitoring with combined direct and indirect methods," *Journal of Applied Remote Sensing*, vol. 1, Article ID 014511, 2020.

[33] J. C. Weinstein, M. Sanayei, and B. R. Brenner, "Bridge damage identification using artificial neural networks," *Journal of Bridge Engineering*, vol. 23, no. 11, Article ID 04018084, 2018.

[34] Y. Xie, C. Gao, P. Wang, L. Zhou, C. Zhang, and X. Qu, "Research on vibration fatigue damage locations of offshore oil and gas pipelines based on the GA-improved BP neural network," *Shock and Vibration*, vol. 2023, Article ID 2530651, 18 pages, 2023.

[35] H. B. Bisheh, G. G. Amiri, and E. Darvishan, "Ensemble classifiers and feature-based methods for structural damage assessment," *Shock and Vibration*, vol. 2020, Article ID 8899487, 14 pages, 2020.

[36] A. Malekjafarian, F. Golpayegani, C. Moloney, and S. Clarke, "A machine learning approach to bridge-damage detection using responses measured on a passing vehicle," *Sensors*, vol. 19, no. 18, p. 4035, 2019.

[37] H. Nick, A. Aziminejad, M. Hamid Hosseini, and K. Laknejadi, "Damage identification in steel girder bridges using modal strain energy-based damage index method and artificial neural network," *Engineering Failure Analysis*, vol. 119, Article ID 105010, 2021.

[38] MathWorks Inc, *MATLAB®, Version 8.0.0.783 (R2012b)*, The MathWorks Inc, Natick, MA, USA, 2012.

[39] B. Peeters, *System identification and damage detection in civil engineering*, Ph.D. Dissertation, Departement Burgerlijke Bouwkunde, Katholieke Universiteit Leuven, Leuven, Belgium, 2000.

[40] J. Kaminski Jr and J. D. Riera, "Structural damage detection by means vibration test," in *Proceedings of the 14th International Conference on Structural Mechanics in Reactor Technology*, SMiRT, Manchester, UK, August, 1997.

[41] G. Zeni, "Detecção de dano em estruturas utilizando identificação modal estocástica e um algoritmo de otimização," Master dissertation, Programa de Pós-Graduação em Engenharia Mecânica, Universidade Federal do Rio Grande do Sul, PROMEC/UFRGS, Porto Alegre, Brazil, 2018.

[42] O. Begambre and J. E. Laier, "A hybrid Particle Swarm Optimization – Simplex algorithm (PSOS) for structural damage identification," *Advances in Engineering Software*, vol. 40, no. 9, pp. 883–891, 2009.

[43] G. D. Roeck, "The state-of-the-art of damage detection by vibration monitoring: the SIMCES experience," *Journal of Structural Control*, vol. 10, no. 2, pp. 127–134, 2003.

[44] B. Peeters and G. De Roeck, "One-year monitoring of the Z24-Bridge: environmental effects versus damage events," *Earthquake Engineering and Structural Dynamics*, vol. 30, no. 2, pp. 149–171, 2001.

[45] C. Krämer, "Brite-Euram Project SIMCES, Task A1 and A2: long term monitoring and bridge tests," Technical report 168'349/20e, EMPA, Dübendorf, Switzerland, 1999.

[46] J. Maeck and G. De Roeck, "Description of Z24 benchmark," *Mechanical Systems and Signal Processing*, vol. 17, no. 1, pp. 127–131, 2003.

[47] E. Reynders and G. De Roeck, "Continuous vibration monitoring and progressive damage testing on the Z24 bridge," *Encyclopedia of Structural Health Monitoring*, pp. 2149–2158, John Wiley & Sons, Hoboken, NJ, USA, 2009.

[48] E. Govahi, M. Salkhordeh, and M. Mirtaheri, "Cyclic performance of different mitigation strategies proposed for segmental precast bridge piers," *Structures*, vol. 36, pp. 344–357, 2022.

[49] Y. Liu, Z. Mei, B. Wu et al., "Seismic behaviour and failure-mode-prediction method of a reinforced-concrete rigid-frame bridge with thin-walled tall piers: investigation by model-updating hybrid test," *Engineering Structures*, vol. 208, Article ID 110302, 2020.

[50] A. Teughels and G. De Roeck, "Structural damage identification of the highway bridge Z24 by FE model updating," *Journal of Sound and Vibration*, vol. 278, no. 3, pp. 589–610, 2004.

[51] E. Reynders, A. Teughels, and G. De Roeck, "Finite element model updating and structural damage identification using OMAX data," *Mechanical Systems and Signal Processing*, vol. 24, no. 5, pp. 1306–1323, 2010.

[52] Ansys, *Ansys®, Academic Research Mechanical, Release 22.2*, ANSYS, Inc, Canonsburg, PA, USA, 2022.

[53] S. Sony, S. Gamage, A. Sadhu, and J. Samarabandu, "Vibration-based multiclass damage detection and localization using long short-term memory networks," *Structures*, vol. 35, pp. 436–451, 2022.

[54] M. G. Masciotta, L. F. Ramos, P. B. Lourenço, M. Vasta, and G. De Roeck, "A spectrum-driven damage identification technique: application and validation through the numerical simulation of the Z24 Bridge," *Mechanical Systems and Signal Processing*, vol. 70-71, pp. 578–600, 2016.